

MOLECULAR STRUCTURE DETERMINES CHEMICAL REACTIVITIES AND, THUS, TRANSFORMATION PATHWAYS

¹Dr. Mohammad (Mo) Qasim*; ²Patricia Honea; ³Dr. Leonard Gorb; ^{1,4}Dr. Jerzy Leszczynski
¹USACE ERDC, 3909 Halls Ferry Rd., Vicksburg, MS 39180; ²U. of Mississippi Medical School, Jackson, MS; ³SpecPro, Inc., Huntsville, AL; ⁴Director, Computational Center for Molecular Structure and Interactions, Jackson State U., Jackson, MS

ABSTRACT

Structural reactivities of a nitroaromatic and heterocyclic nitramines were compared under selected reaction conditions, with 2,4,6-trinitrotoluene (TNT) as the exemplar of nitroaromatic; hexahydro-1,4,5-trinitro-1,3,5-triazine (RDX) and octahydro-1,3,5-tetranitro-1,3,5,7-tetrazocine (HMX) exemplifying the heterocyclic nitramine; and 2,4,6,8,10,12-hexanitrohexaazoisowurtzitane representing cage heterocyclic nitramine explosives. The hypothesis that *molecular structure determines chemical reactivities and transformations* was supported through a combination of computational chemistry (CC) and spectroscopic techniques. This combination of predictive and analytical tools addresses the DoD need for fast and accurate techniques to assess environmental transport and impact of toxicity.

1. INTRODUCTION

1.1 Background

To illustrate the utility of combining CC predictive and analytical capability with spectroscopic and further CC verification: our previous work with CL-20 revealed a transformation product via alkaline hydrolysis to be more toxic and recalcitrant than its parent. Our combination CC and spectroscopic methodology allowed manipulating a competing transformation pathway to become dominant, through application of free radicals generated via monochromatic irradiation—producing a more desirable transformation product [Qasim, 2005]. This research seeks to expand the methodology to other explosive nitro compounds in order to reduce both cost and risk (through avoidance of most on-site experimentation).

1.2. GOAL

To prove/disprove hypothesis, the goal of both CC and experimental approaches was to

correlate reaction rates and mechanisms to molecular structure.

2. APPROACH

i) Structural reactivity reaction mechanisms and rates were studied via CC prediction in which semiempirical (MOPAC) methods were applied to all mentioned energetic compounds

ii) Spectroscopic techniques were used to verify CC results. Initial and selected subsequent steps of reactions were revealed through changes in ultra-violet (UV) and visible (Vis) spectra. Stopped Flow (SF) was used to follow rates of reaction of the alkaline hydrolysis of TNT, RDX, HMX and CL-20. FTIR was used to follow formation of intermediates via changes in functional groups.

Free radical reactions of all mentioned compounds were then accomplished through dark Fenton reactions and through photo-induced free radicals obtained through irradiation at wavelengths of maximum absorption and also at wavelengths generated by resultant reactions.

CL-20 reactions were also performed via disodium disulfite, which can operate both as a reductive and as a free radical generator, depending on conditions, and was expected to act primarily in producing free radicals [Qasim, SAR/QSAR, Vol 16, No. 3, 2005].

iii) Density Functional Theory (DFT) was used to analyze and further predict TNT and CL-20 transformation mechanisms.

RESULTS

Due to its aromatic, planar structure, free radical reactions with TNT, using Fenton reagents and irradiation at 233 nm (wavelength

Report Documentation Page

Form Approved
OMB No. 0704-0188

Public reporting burden for the collection of information is estimated to average 1 hour per response, including the time for reviewing instructions, searching existing data sources, gathering and maintaining the data needed, and completing and reviewing the collection of information. Send comments regarding this burden estimate or any other aspect of this collection of information, including suggestions for reducing this burden, to Washington Headquarters Services, Directorate for Information Operations and Reports, 1215 Jefferson Davis Highway, Suite 1204, Arlington VA 22202-4302. Respondents should be aware that notwithstanding any other provision of law, no person shall be subject to a penalty for failing to comply with a collection of information if it does not display a currently valid OMB control number.

1. REPORT DATE 01 NOV 2006	2. REPORT TYPE N/A	3. DATES COVERED -	
4. TITLE AND SUBTITLE Molecular Structure Determines Chemical Reactivities and, Thus, Transformation Pathways		5a. CONTRACT NUMBER	
		5b. GRANT NUMBER	
		5c. PROGRAM ELEMENT NUMBER	
6. AUTHOR(S)		5d. PROJECT NUMBER	
		5e. TASK NUMBER	
		5f. WORK UNIT NUMBER	
7. PERFORMING ORGANIZATION NAME(S) AND ADDRESS(ES) USACE ERDC, 3909 Halls Ferry Rd., Vicksburg, MS 39180		8. PERFORMING ORGANIZATION REPORT NUMBER	
9. SPONSORING/MONITORING AGENCY NAME(S) AND ADDRESS(ES)		10. SPONSOR/MONITOR'S ACRONYM(S)	
		11. SPONSOR/MONITOR'S REPORT NUMBER(S)	
12. DISTRIBUTION/AVAILABILITY STATEMENT Approved for public release, distribution unlimited			
13. SUPPLEMENTARY NOTES See also ADM002075., The original document contains color images.			
14. ABSTRACT			
15. SUBJECT TERMS			
16. SECURITY CLASSIFICATION OF:			17. LIMITATION OF ABSTRACT
a. REPORT unclassified	b. ABSTRACT unclassified	c. THIS PAGE unclassified	UU
			18. NUMBER OF PAGES 26
			19a. NAME OF RESPONSIBLE PERSON

AM1 and MNDO Energies				
Structure	AM1		MNDO	
	LUMO	HOMO	LUMO	HOMO
RDX	-1.1008	-12.1057	-1.0978	-12.3302
RDX - Mononitroso	-0.8675	-11.3769	-0.8998	-11.6232
RDX - Monohydroxylamine	-0.5772	-11.0252	-0.6948	-11.295
RDX – Monoamino	-0.5534	-10.6059	-0.5381	-11.008
RDX- Nucleophilic OH ⁻ Substitution for NO ₂	-0.648	-11.0344	-0.7573	-11.315
RDX – OH ⁻ Proton Abstraction/NO ₂ Elimination; Formation of C=N	-1.2319	-11.2436	-1.0505	-11.4885
RDX Free Radical Oxidation	-0.9574	-11.4487	-0.9544	-11.7472
RDX with 1 Ring C-N Bond Broken/Formation of Terminal C=N	-1.6718	-11.7426	-1.5424	-11.7478
HMX	-1.1188	-11.7305	-1.046	-12.1415
HMX – Mononitroso	-0.866	-11.2678	-0.887	-11.5792
HMX - Monohydroxylamine	-0.9456	-10.219	-0.8289	-11.3209
HMX – Monoamino	-0.9832	-10.5952	-0.801	-11.0598
HMX – Nucleophilic OH ⁻ Substitution for NO ₂	-0.7085	-10.9846	-0.7291	-11.3224
HMX – OH ⁻ Proton Abstraction/NO ₂ Elimination; Formation of C-N ???	-1.181	-11.3271	-1.2604	-11.7951
HMX with 1 Ring C-N Bond Broken	-1.087	-11.3931	-1.1171	-11.71
CL-20	-2.304	-12.2423	-2.0466	-12.5675
CL-20 – Mononitroso	-2.1116	-11.9888	-1.9569	-12.2391
CL-20 – Monohydroxylamine	-1.9884	-11.5847	-1.808	-11.9457
CL-20 – NO ₂ + OH ⁻ Nucleophilic Substitution	-1.9908	-11.7158	-1.8495	-11.9125
CL-20 OH - Proton Abstraction/NO ₂ Elimination; Formation of C=N	-3.1231	-11.8908	-3.0378	-12.263
CL-20 with 1 Broken C-C Bond	-2.4269	-12.0484	-2.431	-12.4485
CL-20 with 2 Broken C-C Bonds	-1.4168	-11.0833	-2.0537	-12.3457
ONC	-3.0988	-13.5375	-3.153	-13.3486
ONC with 1 Broken C-C Bond	-3.0304	-13.5147	-3.0987	-13.2056
ONC with 1 Nitro Group Removed	-2.8644	-13.3562	-2.9212	-13.1724
ONC with OH ⁻ Substituted for NO ₂	-2.844	-13.2014	-2.9143	-13.0764
ONC with 1 NO ₂ and 1 C-C Removed	-2.7548	-13.2942	-2.8201	-13.1319
TNTAC	-2.781	-13.1054	-2.5788	-13.0383
TNTAC with OH ⁻ Substituted for NO ₂	-2.2686	-12.5495	-2.1981	-12.7059
TNTAC minus NO ₂ (2,4,6 Trinitro-1,3,5,7-tetrazacubane)	-2.1448	-12.6956	-2.1202	-12.7683
TNTAC with Broken Cage C-N Bond	-2.5648	-12.4589	-2.3394	-12.7458

Table 1. SEMIEMPIRICAL COMPARISON OF NITRAMINE (RDX AND HMX) AND CAGE NITRO (ONC) AND CAGE NITRAMINE (CL-20 AND TNTAC) ENERGETIC COMPOUNDS AND SELECTED DERIVATIVES [Generated for this research]

This comparison shows definite AM1 and MNDO HOMO/LUMO trends. ONC and TNTAC are not dealt with specifically elsewhere in this paper due to the lack of physical availability of ONC and to TNTAC not yet being synthesized, but are shown here to further indicate general trends.

Illustrated general trends:

i) The less polar, more symmetrical, and more carbon-carbon (C-C) bonds, the lower are the HOMO and LUMO energies;

ii) The more crowded the compound—due to increase in number of nitro groups—the lower are the HOMO/LUMO energies;

iii) Lower polarity, greater symmetry, higher number of C-C bonds render these compounds more susceptible to free radical bond-breaking than to alkali hydrolysis;

iv) The parent compound generally has lower HOMO/LUMO energies than their various derivatives.

of maximum absorption) did not produce significant UV/Vis spectral changes [Qasim, 2004; Qasim, *SAR/QSAR*, Vol 16, No. 5, 2005].

Irradiation alone of TNT at 233 nm produced no change whatsoever, Fig.1 (unpublished figure) [Qasim, 2004; Qasim, *SAR/QSAR* Vol. 16, No. 5, 2005].

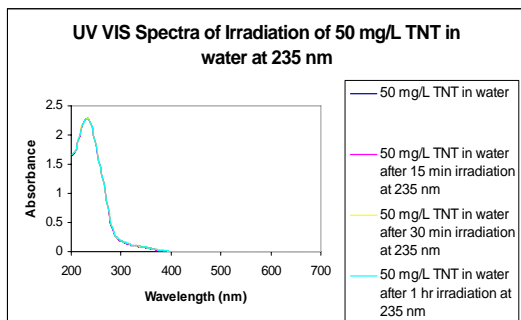


Figure 1. TNT shows no change upon irradiation

Irradiation alone of CL-20 at 236 nm (wavelength of maximum absorption) produced dramatic change in that i) complete disappearance of its UV spectra occurred as well as the ii) appearance of a sharp, high-intensity peak at lower wavelength—the latter a characteristic of low molecular weight compounds and identical to that of imidazole. A similar peak appeared upon irradiation of RDX, Fig. 2. (similar to one from Qasim, *SAR/QSAR*, Vol 16, No. 5, 2005) [Kholod, 2006; Okovytyy, 2005] A CC and spectroscopic study of this compound is currently underway.

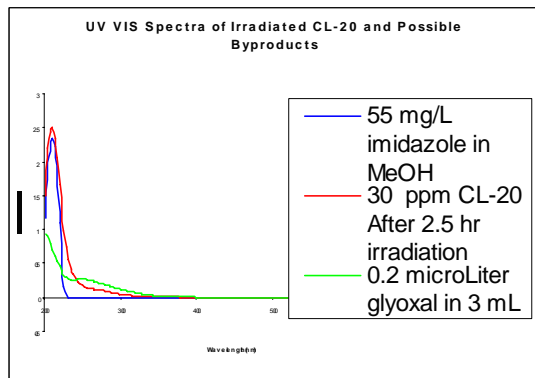


Figure 2. Reveals the sharp, high intensity “imidazole like” peak

Disappearance of the band upon irradiation of CL-20 photo-induced free radical reactions at 370 nm, where the conjugated pi system of the aromatic intermediate absorbs, indicates transformation by photo-induced free-radical reactions Qasim, *SAR/QSAR*, Vol 16, No. 3, 2005; *SAR/QSAR*, Vol 16, No. 5, 2005].

Upon irradiation of CL-20 at 420 nm, at low concentration of sodium hydroxide (NaOH), the peak disappears. However, upon irradiation at 420 nm at high NaOH concentration, the peak shifts back to 370 nm. Upon further addition of OH⁻ to CL-20, the Vis spectra shifts back to a shorter wavelength, indicating formation of a smaller molecule—possibly due to the removal of an imidazole ring, forming a two-ring aromatic compound *SAR/QSAR*, Vol 16, No. 3, 2005; *SAR/QSAR*, Vol 16, No. 5, 2005].

RDX and HMX required high concentrations of hydroxide ions (OH⁻) to effect transformation, Figs 3 and 4. Transformation of HMX via OH⁻ was slower than that of RDX due to HMX being a larger compound and possibly to other structural characteristics [*SAR/QSAR*, Vol 16, No. 5, 2005].

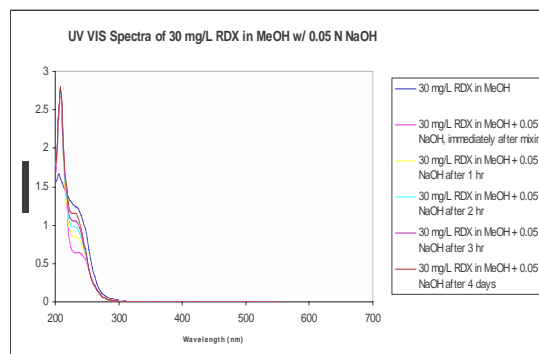


Figure 3. Low concentration of NaOH does not transform RDX completely.

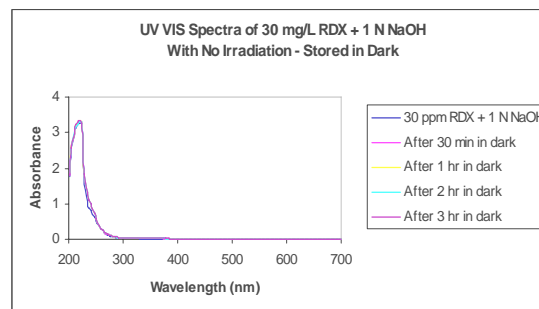


Figure 4. RDX transformation required a high concentration of NaOH.

In addition to UV/Vis data, SF data also shows the transformation of HMX via alkaline hydrolysis to be slower than that of RDX and that higher concentrations of NaOH were required to effect the transformation of both RDX and HMX [SAR/QSAR, Vol 16, No. 3, 2005].

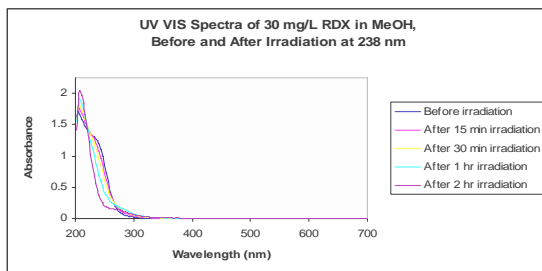


Figure 5. Shows RDX transformation via both alkaline hydrolysis and photolysis (irradiation at the RDX wavelength of maximum absorption) [unpublished]

Fig 5. reveals the enhancement of degradation accomplished by the addition of free-radical reactions generated via monochromatic irradiation to those occurring via alkaline hydrolysis. This enhancement is expected because irradiation of both RDX and HMX at their respective wavelengths of maximum absorption effect total transformation [Qasim, SAR/QSAR, Vol. 16, No. 3, 2005].

With all compounds, UV spectral changes due to dark Fenton free radical reactions were not as significant as those via irradiation [unpublished data].

SF data shows that CL-20 treated with disodium disulfite transforms in a similar manner to that with free radicals generated through irradiation but at a much slower rate. It is posited that transformation may occur through breaking of the disodium disulfite sulfur-sulfur bond, thus generating .SO₂ free radicals.

CONCLUSIONS

i) For maximum robustness and lowest toxicity, chemical transformation techniques must be selected according to the molecular structure of the compound to be transformed. For example, transformation of CL-20 via high alkaline concentrations leads to a toxic pyrazine, whereas transformation via photo-induced free

radical reactions at 236 nm leads to formation of a peak of high absorptivity at a wavelength lower than that of the parent—indicating an alternative CL-20 transformation mechanism [Kholod, 2006; Qasim SAR/QSAR Vol. 16, No. 3, 2005].

ii) Whereas alkaline hydrolysis methods are generally effective for TNT transformation (and that of other nitroaromatic compounds), photolysis and dark Fenton generation of free radical reactions is not effective

iii) From HOMO/LUMO trends, it was noted that less polar, more symmetrical, and higher C-C bonds correlate with lower HOMO/LUMO values, as did crowded compounds resulting from an increased number of nitro groups—rendering them more susceptible to reactions, particularly to free radical reactions as opposed to alkaline hydrolysis driven ones.

iv) Experimental findings correlated well with computational predictions—suggesting that prediction of transformation mechanisms plus lab verification as to feasibility, followed by computational analysis of total results, constitutes an excellent tool for investigating transformations of current explosives, emerging military compounds and their various impacts on the environment.

ACKNOWLEDGEMENTS

The semiempirical and spectroscopic experiments were conducted at the U. S. Army Environmental Quality Technology program at the USACE Engineer Research and Development Center (ERDC), Environmental Laboratory, Vicksburg, MS. DFT studies were completed at the Computational Center for Molecular Structure and Interactions (CCMSI), Jackson State University, MS.

We thank Dr. John Cullinane, ERDC Technical Director for Military Environmental Engineering and Science; and Dr. Richard E. Price, Environmental Division Branch Chief for their support of this research.

REFERENCES

R. Bajpai, D. Parekh, S. Herrmann, M. Popović, J. Paca, M. Qasim; "A kinetic model of aqueous-

phase alkali hydrolysis of 2,4,6-trinitrotoluene,”
J. Haz. Materials 106B (2004) 55-66.

Y. Kholod, S. Okovytyy, G. Kuramshina, M. Qasim, P. Honea, J. Furey, H. Fredrickson, J. Leszczynski, “Are 1,5- and 1,7-dihydroimidazo[4,5-b:4',5'-e]pyrazine the main products of 2,4,6,8,10,12-hexanitro-2,4,6,8,10,12hexaazaisowurtzitane (CL-20) alkali hydrolysis? A DFT Study of Vibrational Spectra,,” *Journal of Molecular Structure* 794 (2006) 288-302.

S. Okovytyy, Y. Kholod, M. Qasim, H. Frederickson, J. Leszczynski “The Mechanism of Unimolecular Decomposition of CL-20 (2,4,6,8,10,12 Hexanitro-2,4,6,8,10,12-Hexaazaisowurtzitane). A Computational DFT Study,” *Journal of Physical Chemistry A* , 2005, 109, 2964-2970.

M. Qasim, J. Furey, H. Fredrickson, J. Szecsody, C. McGrath, R. Bajpai, “Semi empirical Predictions of Chemical Degradation Reaction Mechanisms of CL-20 as Related to Molecular Structure,” *Structuiral Chemistry*, Vol. 15, No. 5, 10/04.

M. Qasim, H. Fredrickson, C. McGrath, J. Furey, R. Bajpai; “Theoretical Predictions of Chemical Degradation Reaction Mechanisms of RDX and Other Cyclic Nitramines Derived from Their Molecular Structures,” *SAR/QSAR in Environmental Reearch*, Vol. 16, No. 3, 2005, 1-17.

M. Qasim, H. Fredrickson, P. Honea, J. Furey, J. Leszczynski, S. Okovytyy, J. Szecsody, Y. Kholod; “Prediction of CL-20 Chemical Degradation Pathways, Theoretical and Experimental Evidence for Dependence on Competing Modes of Reaction,” *SAR and QSAR in Environmental Research*, Vol. 16, No. 5, 10/05, 493-515.



Molecular Structure Determines Chemical Reactivities and, Thus, Transformation Pathways

25th Army Science Conference
Orlando, Florida
November 27-30, 2006

Dr. Mohammad (Mo) Qasim¹, POC; Patricia Honea²; Dr.
Leonid Gorb^{1,3}; Dr. Jerzy Leszczynski^{1,4}

¹USACE ERDC EL, Vicksburg, MS; ²University of Mississippi
Medical School; ³SpecPro, Inc.; ⁴Director, Computational
Center for Molecular Structure and Interactions, Jackson
State University





Hypothesis: *Molecular structure determines chemical reactivities and transformations*

Goal: Correlate reaction rates and mechanisms to molecular structure

Purpose: Address DoD need for fast, accurate, cost-effective, low-risk methods to assess environmental impacts thru avoidance of most on-site experimentation

Method: combined computational chemistry and spectroscopy

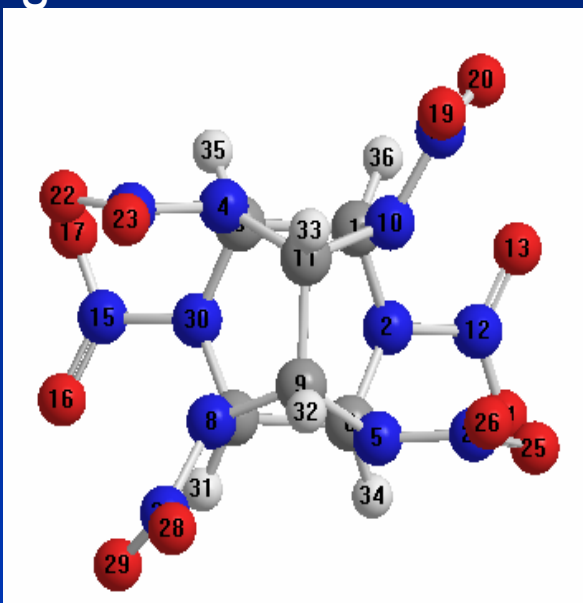


CL-20 Bond Lengths and Charges

Bond Length

Atom Charge

Development Center



N(2)-C(1)	1.4641
C(3)-C(1)	1.6275
C(1)-N(10)	1.5091
C(1)-H(36)	1.1353
N(2)-C(6)	1.4669
N(2)-N(12)	1.4182
N(4)-C(3)	1.4939
C(3)-N(30)	1.4670
C(3)-H(35)	1.1326
N(4)-C(11)	1.4899
N(4)-N(21)	1.4023
C(6)-N(5)	1.4940
N(5)-C(9)	1.4900
N(5)-N(24)	1.4023
C(6)-C(7)	1.6274
C(6)-H(34)	1.1326
N(8)-C(7)	1.5091
C(7)-N(30)	1.4641
H(31)-C(7)	1.1354
N(8)-C(9)	1.4847
N(8)-N(27)	1.4221
C(9)-C(11)	1.6161
C(9)-H(32)	1.1343
N(10)-C(11)	1.4847
N(10)-N(18)	1.4219
H(33)-C(11)	1.1343
O(13)-N(12)	1.1948
O(14)-N(12)	1.1936
N(15)-O(16)	1.1949
N(15)-O(17)	1.1936
N(30)-N(15)	1.4181

C (1)	0.06113
N (2)	-0.36998
C (3)	0.06072
N (4)	-0.37073
N (5)	-0.37115
C (6)	0.05949
C (7)	0.06041
N (8)	-0.34008
C (9)	0.01150
N (10)	-0.34298
C (11)	0.01011
N (12)	0.70911
O (13)	-0.36123
O (14)	-0.37274
N (15)	0.71109
O (16)	-0.36781
O (17)	-0.37156
N (18)	0.70532
O (19)	-0.37628
O (20)	-0.37203
N (21)	0.69559
O (22)	-0.38390
O (23)	-0.37915
N (24)	0.69386
O (25)	-0.38857
O (26)	-0.37522
N (27)	0.70396
O (28)	-0.37678
O (29)	-0.37445
N (30)	-0.36565

US Army



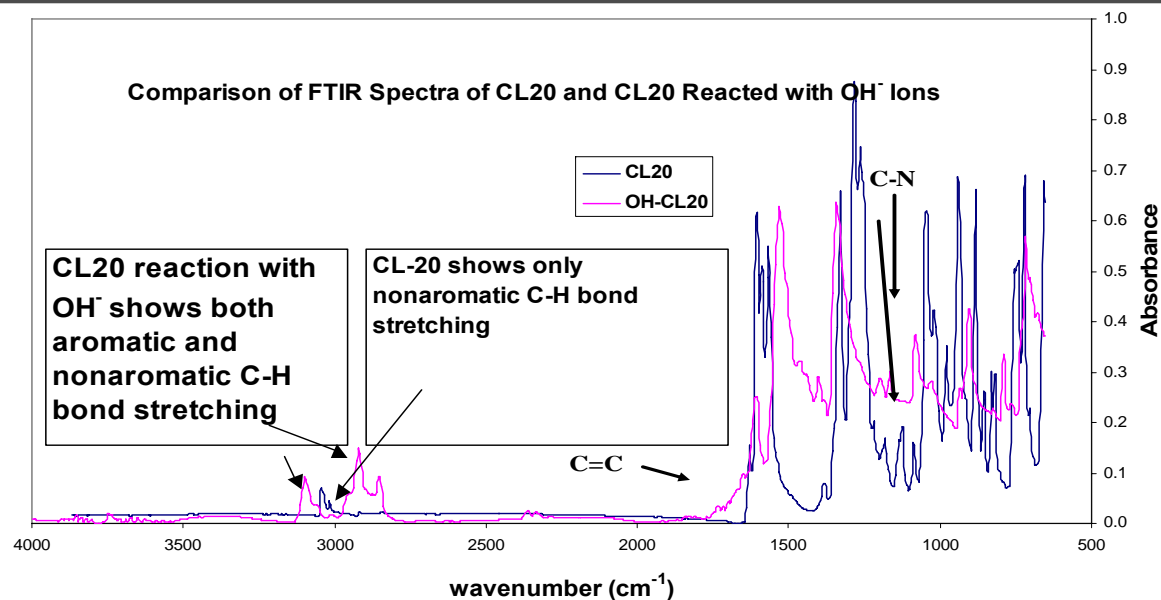
One Corps, One Regim

So



JR

FTIR Spectra Show Two Competing Transformation Mechanisms for CL-20 at Low and High Alkaline Concentrations



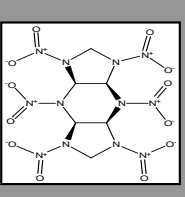
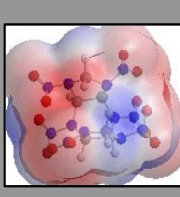
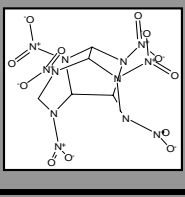
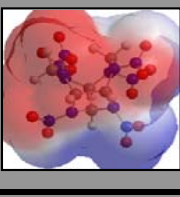
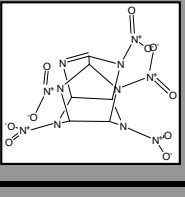
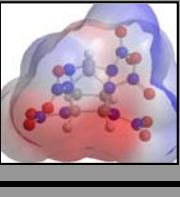
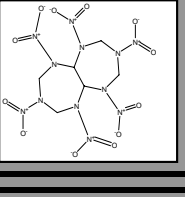
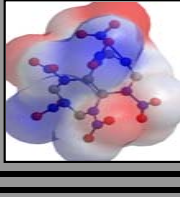
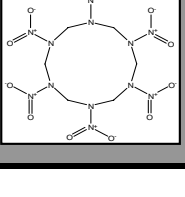
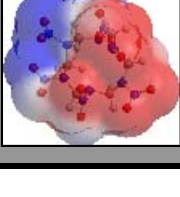
At higher hydroxide ion concentration (1.0 N:1000 ppm of CL-20), the FTIR spectra shows that most of the C-H stretching is more than 3000 cm⁻¹, indicating the formation of an aromatic intermediate with a C=C bond – similar to that in TNT. A decrease in C-N at 1049 cm⁻¹ is also noted.

FTIR data show that at lower hydroxide ion concentration (less than 2:1 molar ratio of OH⁻ to CL-20), the resulting C-H bond stretching is mostly aliphatic (peak at less than 3000 cm⁻¹)



Progressive derivation of most likely transformations of CL-20 and investigation of most likely bond-breaking sites (Steric and Formation=Kcal/mole , Homo and Lumo= eV)

US Army Engineer Research & Development Center

 	CL-20 with attic C-C bond broken	AM1	MNDO	PM3
	Heat of Formation (Kcal/mole)	262.02758	229.65301	108.28103
	HOMO (82) (eV)	-11.87	-12.43	-11.41
	LUMO (83) (eV)	-2.06	-1.96	-1.38
 	CL-20 with one base C-C broken	AM1	MNDO	PM3
	Heat of Formation	277.86939	260.98049	125.20087
	HOMO (82)	-11.84	-12.31	-11.24
	LUMO (83)	-2.22	-2.25	-1.61
 	CL-20 with one nitro group removed	AM1	MNDO	PM3
	Heat of Formation	333.26126	273.41153	163.53663
	HOMO (72)	-12.13	-12.27	-11.44
	LUMO (73)	-3.2	-3.03	-2.46
 	CL-20 with both base C-C broken	AM1	MNDO	PM3
	Heat of Formation	496.56925	467.75493	318.23249
	HOMO (78)	-10.92	-11.3	-10.04
	LUMO (79)	-3.06	-3.09	-2.42
 	CL-20 with all three C-C broken	AM1	MNDO	PM3
	Heat of Formation	230.78293	238.6664	100.22208
	HOMO (84)	-11.76	-12.19	-11.21
	LUMO (85)	-1.55	-1.61	-1.14



One Corps, One Regiment, One Team . . . Serving Soldiers, the Army, the Nation



Progressive derivation of most likely transformations of CL-20 and investigation of most likely bond-breaking sites
(Steric and Formation=Kcal/mole , Homo and Lumo= eV)

ATTIC	LUMO	HOMO	GAP	Steric	H _F
Cl-20	-2.23	-12.16	9.93	40.16	277.95
Cl-20 with one nitro group removed	-3.19	-12.14	8.95	33.67	333.40
Cl-20 with two nitro groups removed	-3.55	-11.92	8.37	68.46	402.61
Cl-20 with attic C-C broken and 2 nitro groups removed	-1.63	-11.62	9.99	99.12	229.65
Cl-20 with attic C-C broken and 3 nitro groups removed	-1.92	-11.82	9.90	9.93	238.96
Cl-20 with attic C-C broken and 4 nitro groups removed	-1.97	-11.03	9.06	19.97	225.41
Cl-20 with attic C-C broken and 5 nitro groups removed	-1.48	-10.37	8.89	19.48	188.04
Cl-20 with attic C-C broken and all nitro groups removed	-0.65	-9.87	9.22	22.61	151.74
Pyrazine	-3.28	-10.78	7.50	27.69	229.43
ONE BASE	LUMO	HOMO	GAP	Steric	H _F
Cl-20	-2.23	-12.16	9.93	40.16	277.95
Cl-20 with one base C-C broken	-2.31	-12.06	9.75	62.34	275.54
Cl-20 with 1 base C-C broken and 1 nitro group removed	-2.25	-11.89	9.64	21.15	251.42
Cl-20 with 1 base C-C broken and 2 nitro groups removed	-2.35	-11.80	9.45	86.32	273.49
Cl-20 with 1 base C-C broken and 3 nitro groups removed	-2.63	-11.39	8.76	34.29	289.94
Cl-20 with 1 base C-C broken and 4 nitro groups removed	-2.63	-11.28	8.65	50.83	295.16
Cl-20 with 1 base C-C broken and 5 nitro groups removed	-1.82	-9.61	7.79	102.67	222.30
Cl-20 with 1 base C-C broken and 6 nitro groups removed	-3.33	-10.73	7.40	130.44	283.22
Cl-20 with 2 base C-C broken and 6 nitro groups removed	-1.96	-10.44	8.48	57.60	182.28
Cl-20 with all C-C broken and all 6 nitro groups removed	-1.40	-9.78	8.38	51.29	170.29

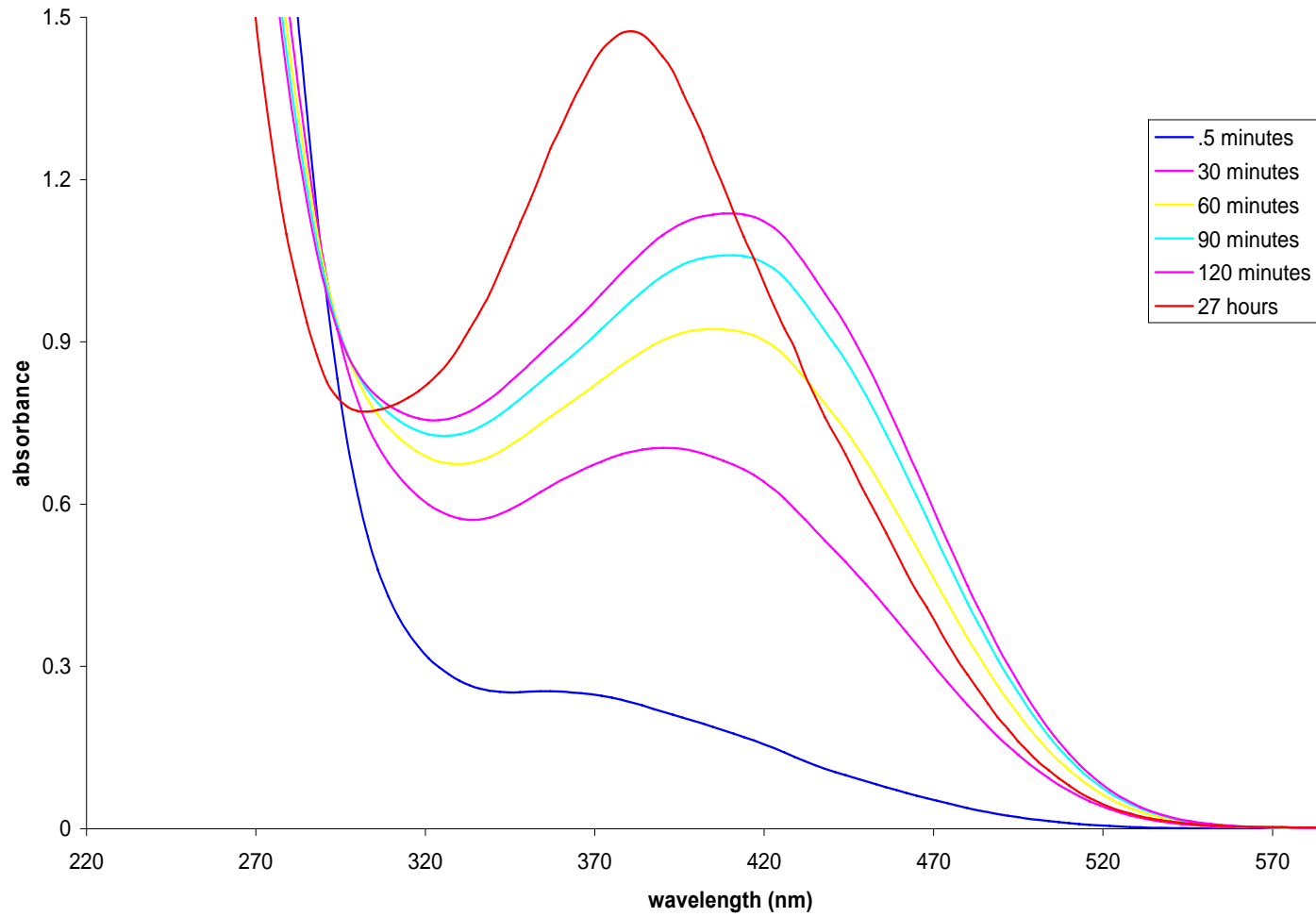


Progressive derivation of most likely transformations of CL-20 and investigation of most likely bond-breaking sites

ONE BASE ALTERNATE	LUMO	HOMO	GAP	Steric	H _F
CI-20	-2.23	-12.16	9.93	40.16	277.95
CI-20 with one base C-C broken	-2.31	-12.06	9.75	62.34	275.54
CI-20 with 1 base C-C broken and 1 nitro group removed	-2.25	-11.89	9.64	21.15	251.42
CI-20 with 1 base C-C broken and 2 nitro groups removed	-2.35	-11.80	9.45	86.32	273.49
CI-20 with 1 base C-C broken and 3 nitro groups removed	-2.63	-11.39	8.76	34.29	289.94
CI-20 with 2 C-C (attic & base) broken and 3 nitro groups removed	-1.89	-10.99	9.10	-10.15	211.00
CI-20 with 3 C-C broken and 3 nitro groups removed	-1.80	-11.17	9.37	-8.19	211.63
CI-20 with 3 C-C broken and 4 nitro groups removed	-1.09	-10.69	9.60	56.13	177.99
CI-20 with 3 C-C broken and 5 nitro groups removed	-1.25	-10.16	8.91	33.09	171.40
CI-20 with all nitro groups removed and C-C broken	-2.39	-10.72	8.33	38.57	331.46
BOTH BASES	LUMO	HOMO	GAP	Steric	H _F
CI-20	-2.23	-12.16	9.93	40.16	277.95
CI-20 with two base C-C bonds broken	-3.14	-10.91	7.77	-1.43	499.90
CI-20 with two base C-C broken and 1 nitro group removed	-1.90	-11.59	9.69	17.81	243.37
CI-20 with two base C-C broken and 2 nitro groups removed	-3.72	-10.72	7.00	-23.26	475.55
CI-20 with two base C-C broken and 3 nitro groups removed	-3.04	-7.12	4.08	-2.04	440.81
CI-20 with two base C-C broken and 4 nitro groups removed	-3.05	-10.20	7.15	-4.52	422.28
CI-20 with two base C-C broken and 5 nitro groups removed	-3.70	-6.25	2.55	16.71	1344.30
CI-20 with two base C-C broken and 6 nitro groups removed	-3.09	-10.66	7.57	98.01	357.99
CI-20 with all C-C broken and all 6 nitro groups removed	-2.39	-10.72	8.33	38.57	331.46

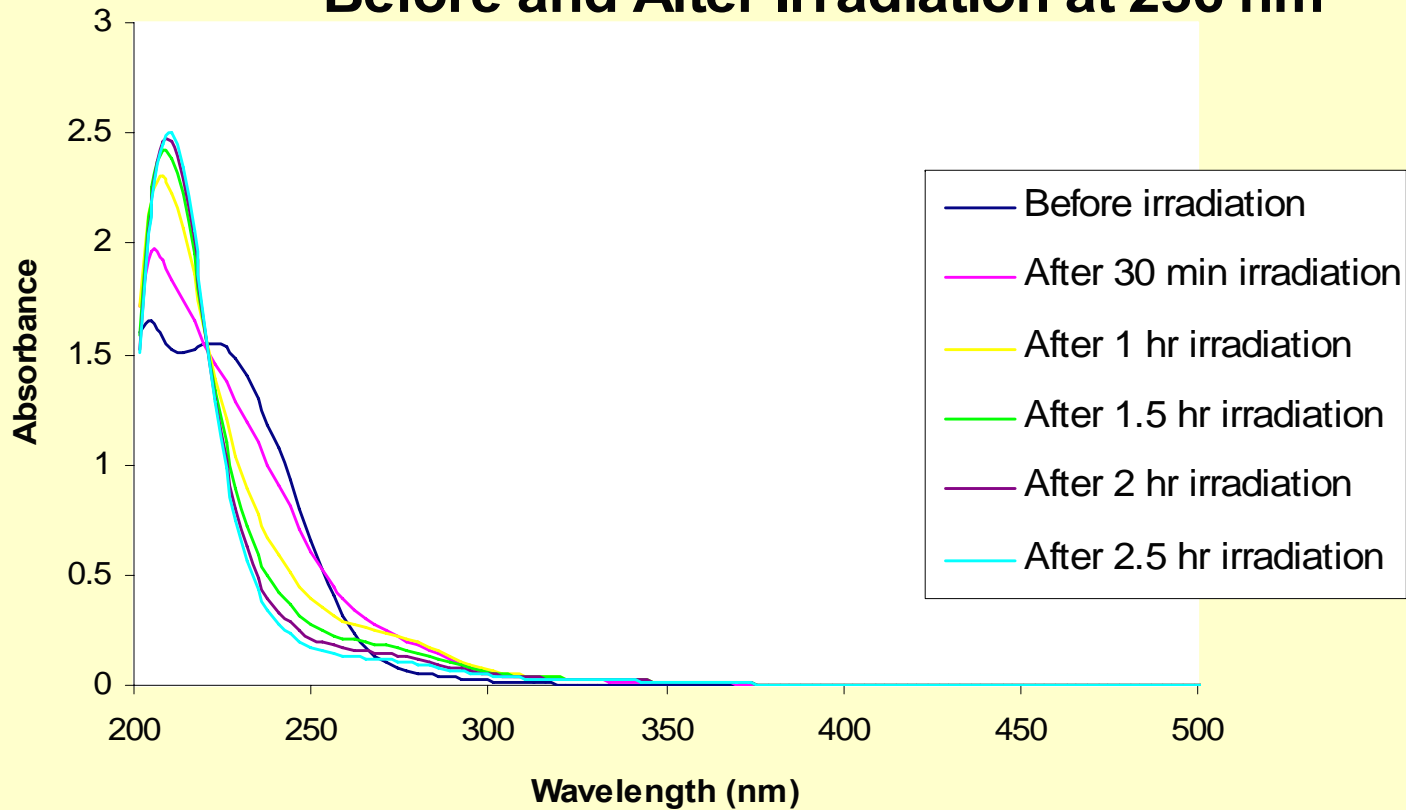


absorbance of mixture of 1 mL of 220 mg/L CL20/MeOH with 1 mL .03 N NaOH solution at times after mixing



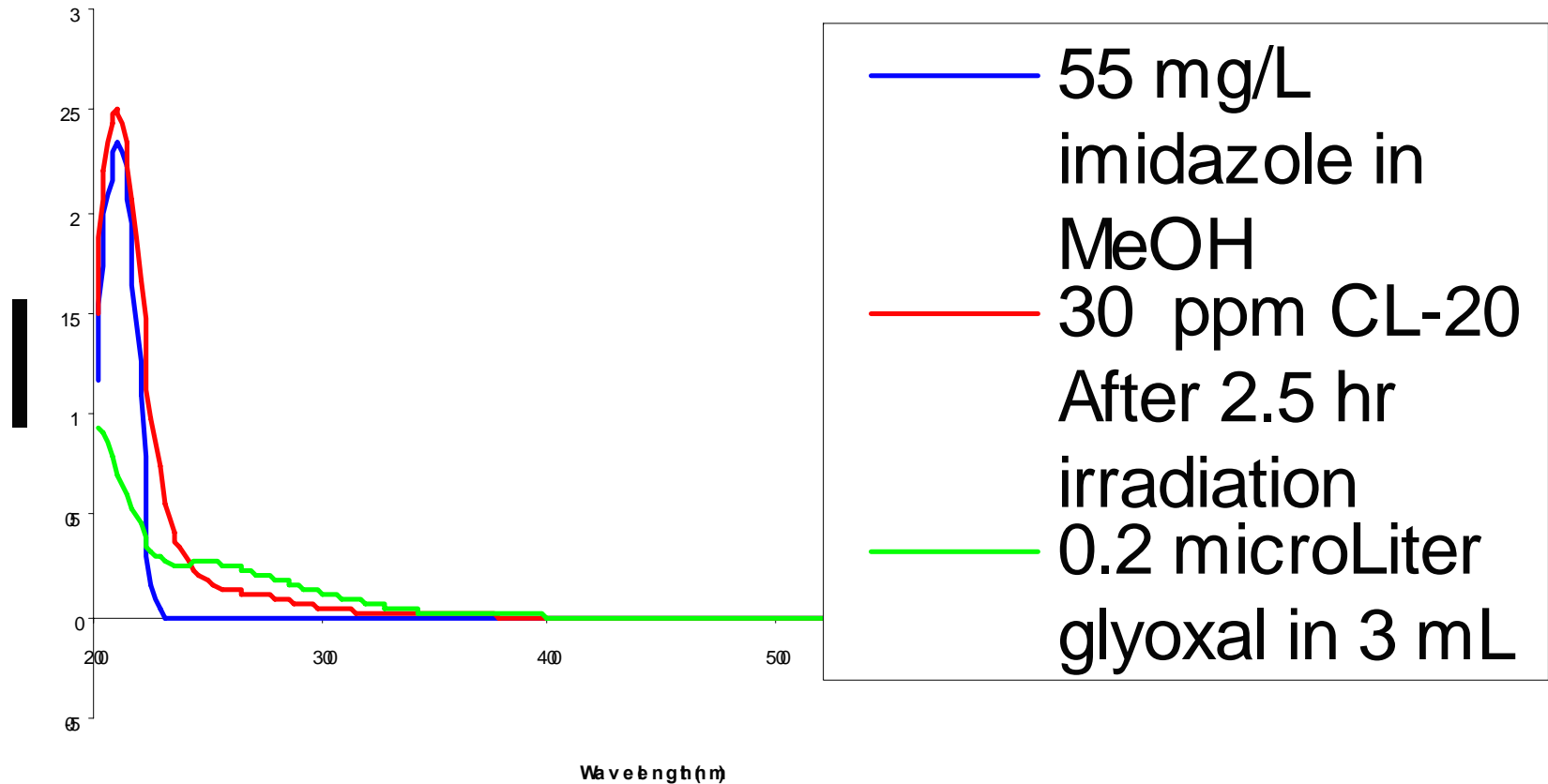


UV VIS Spectra of 30 mg/L CL-20 in MeOH, Before and After Irradiation at 236 nm



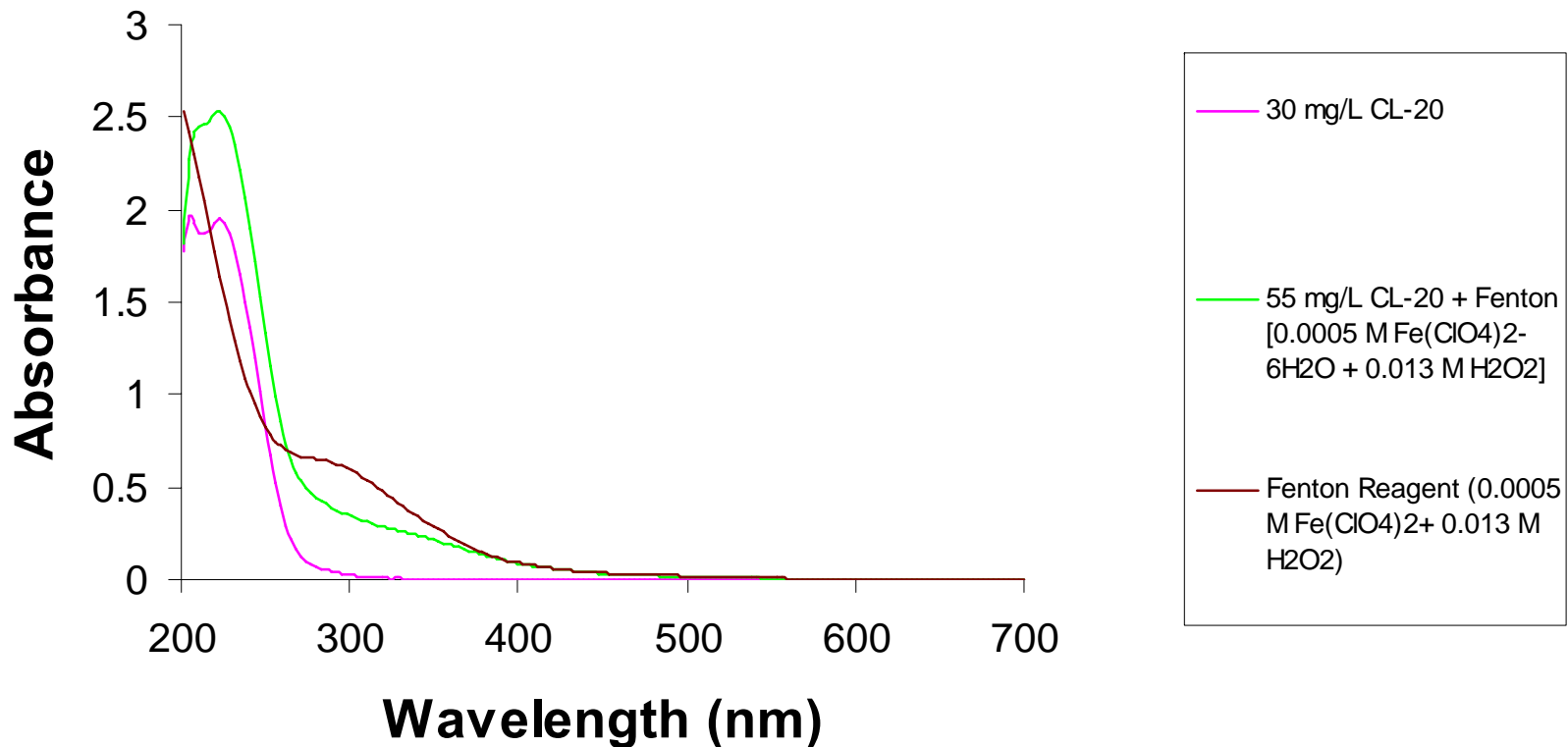


UV VIS Spectra of Irradiated CL-20 and Possible Byproducts





UV/VIS of CL-20 + Fenton



Homo and Lumo Energies (ev) of Selected Caged and Cyclic Nitro Compounds

AM1 and MNDO Energies

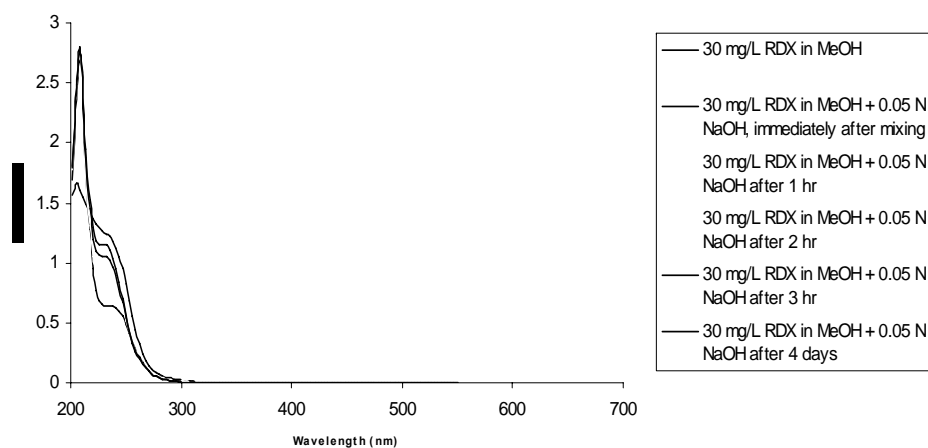
Structure	AM1		MNDO	
	LUMO	HOMO	LUMO	HOMO
RDX	-1.1008	-12.1057	-1.0978	-12.3302
RDX - Mononitroso	-0.8675	-11.3769	-0.8998	-11.6232
RDX - Monohydroxylamine	-0.5772	-11.0252	-0.6948	-11.295
RDX - Monoamino	-0.5534	-10.6059	-0.5381	-11.008
RDX- Nucleophilic OH⁻ Substitution for NO₂	-0.648	-11.0344	-0.7573	-11.315
RDX - OH⁻ Proton Abstraction/NO₂ Elimination; Formation of C=N	-1.2319	-11.2436	-1.0505	-11.4885
RDX Free Radical Oxidation	-0.9574	-11.4487	-0.9544	-11.7472
RDX with 1 Ring C-N Bond Broken/Formation of Terminal C=N	-1.6718	-11.7426	-1.5424	-11.7478
HMX	-1.1188	-11.7305	-1.046	-12.1415
HMX - Mononitroso	-0.866	-11.2678	-0.887	-11.5792
HMX - Monohydroxylamine	-0.9456	-10.219	-0.8289	-11.3209
HMX - Monoamino	-0.9832	-10.5952	-0.801	-11.0598
HMX - Nucleophilic OH⁻ Substitution for NO₂	-0.7085	-10.9846	-0.7291	-11.3224
HMX - OH⁻ Proton Abstraction/NO₂ Elimination; Formation of C-Ndouble bond	-1.181	-11.3271	-1.2604	-11.7951
HMX with 1 Ring C-N Bond Broken	-1.087	-11.3931	-1.1171	-11.71
CL-20	-2.304	-12.2423	-2.0466	-12.5675
CL-20 - Mononitroso	-2.1116	-11.9888	-1.9569	-12.2391
CL-20 - Monohydroxylamine	-1.9884	-11.5847	-1.808	-11.9457
CL-20 - NO₂ + OH⁻ Nucleophilic Substitution	-1.9908	-11.7158	-1.8495	-11.9125
CL-20 OH - Proton Abstraction/NO₂ Elimination; Formation of C=N	-3.1231	-11.8908	-3.0378	- 12.263
CL-20 with 1 Broken C-C Bond	-2.4269	-12.0484	-2.431	-12.4485
CL-20 with 2 Broken C-C Bonds	-1.4168	-11.0833	-2.0537	-12.3457
ONC	-3.0988	-13.5375	-3.153	-13.3486
ONC with 1 Broken C-C Bond	-3.0304	-13.5147	-3.0987	-13.2056
ONC with 1 Nitro Group Removed	-2.8644	-13.3562	-2.9212	-13.1724
ONC with OH⁻ Substituted for NO₂	-2.844	-13.2014	-2.9143	-13.0764
ONC with 1 NO₂ and 1 C-C Removed	-2.7548	-13.2942	-2.8201	-13.1319
TNTAC	-2.781	-13.1054	-2.5788	-13.0383
TNTAC with OH⁻ Substituted for NO₂	-2.2686	-12.5495	-2.1981	-12.7059
TNTAC minus NO₂ (2,4,6 Trinitro-1,3,5,7-tetrazacubane)	-2.1448	-12.6956	-2.1202	-12.7683
TNTAC with Broken Cage C-N Bond	-2.5648	-12.4589	-2.3394	-12.7458



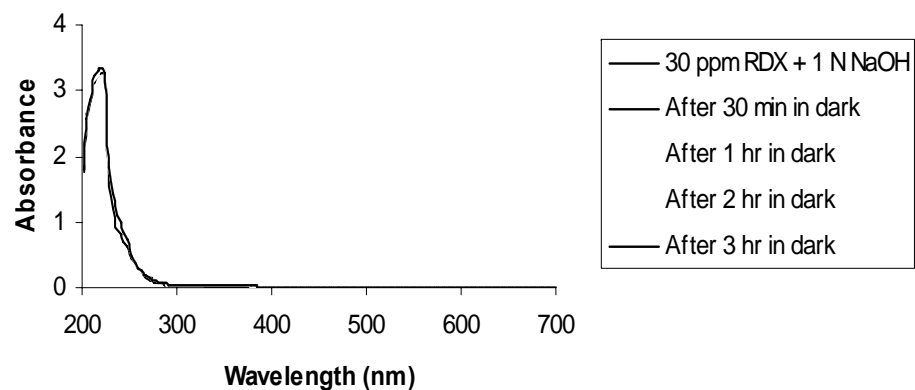


Alkaline hydrolysis Of RDX and HMX

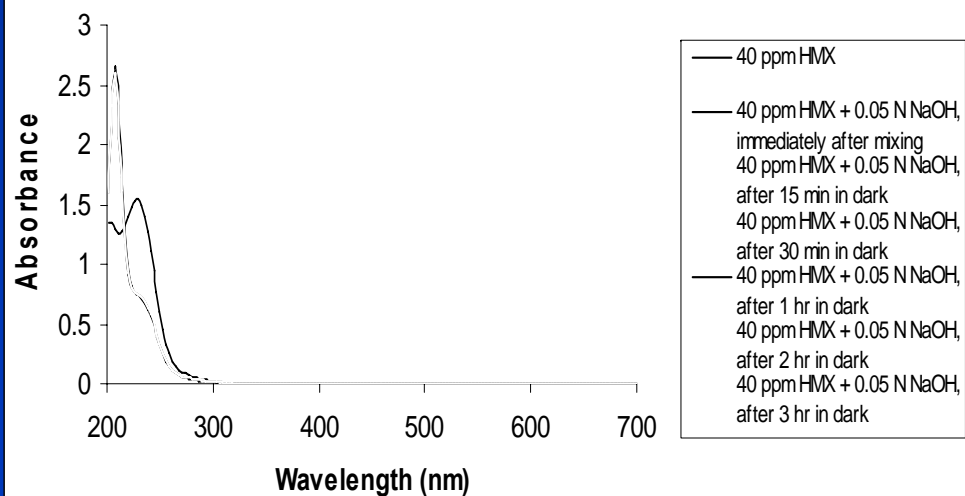
UV VIS Spectra of 30 mg/L RDX in MeOH w/ 0.05 N NaOH



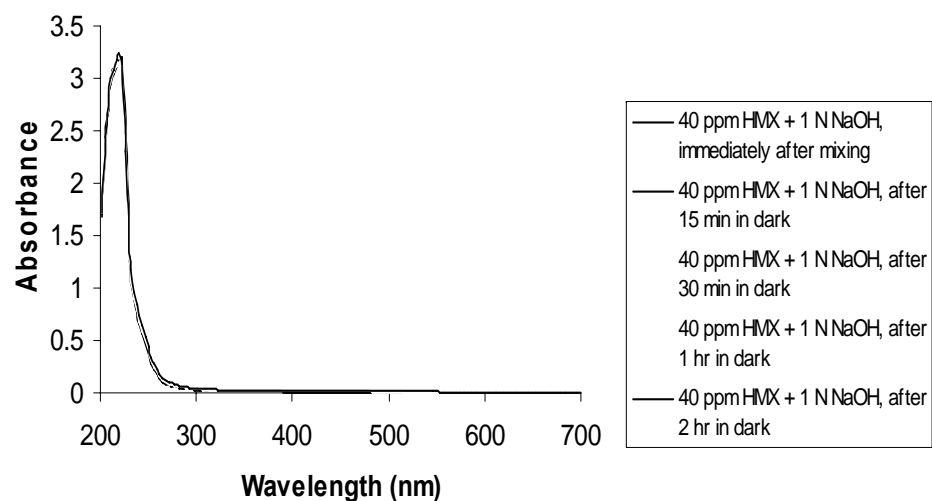
UV VIS Spectra of 30 mg/L RDX + 1 N NaOH
With No Irradiation - Stored in Dark



UV VIS Spectra of 40 ppm HMX + 0.05 N NaOH



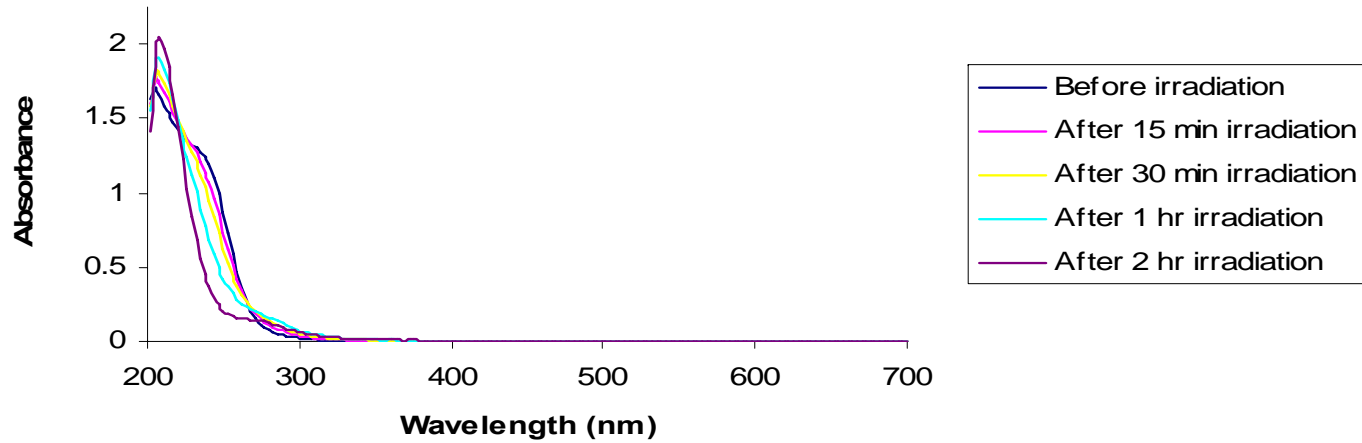
UV VIS Spectra of 40 ppm HMX + 1 N NaOH



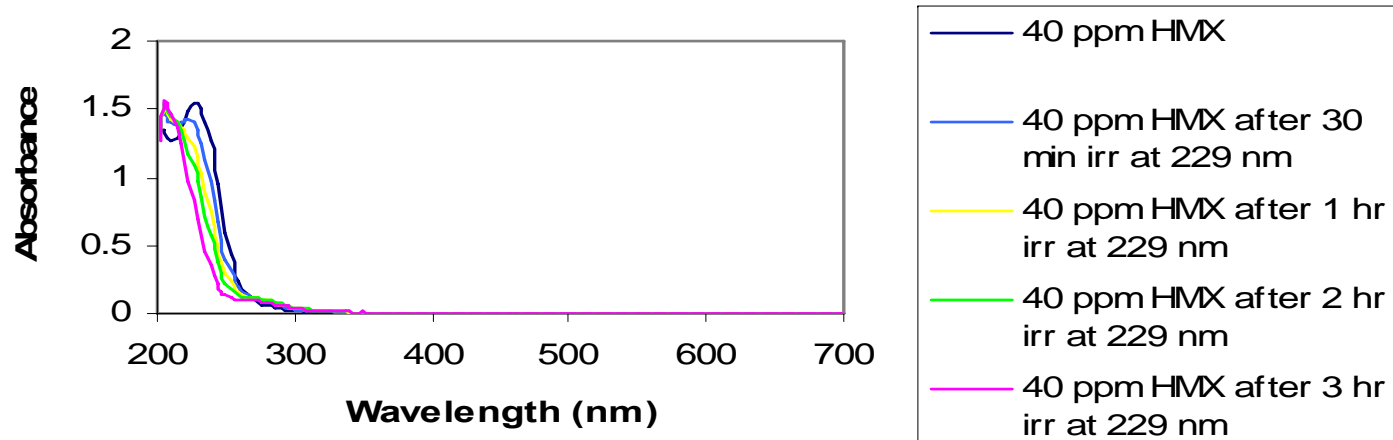


Irradiation of RDX or HMX alone

UV VIS Spectra of 30 mg/L RDX in MeOH, Before and After Irradiation at 238 nm



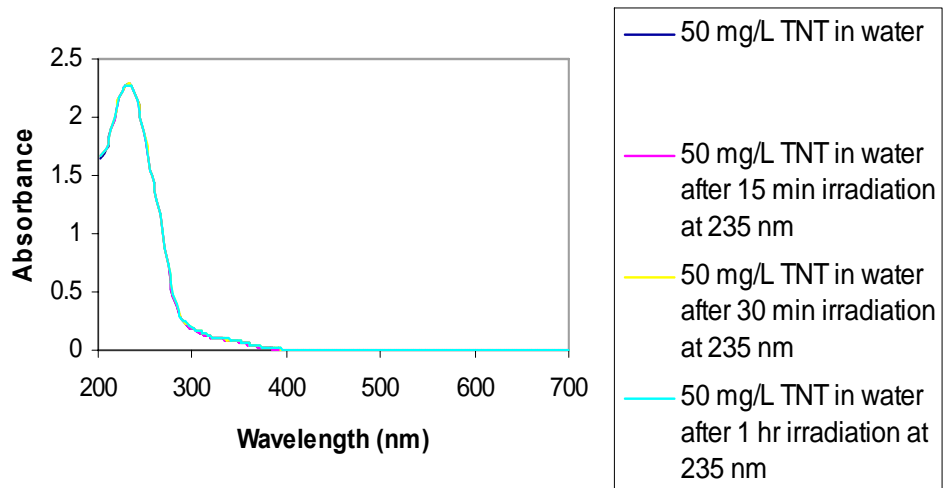
UV VIS Spectra of Irradiation of 40 mg/L HMX in MeOH at 229 nm



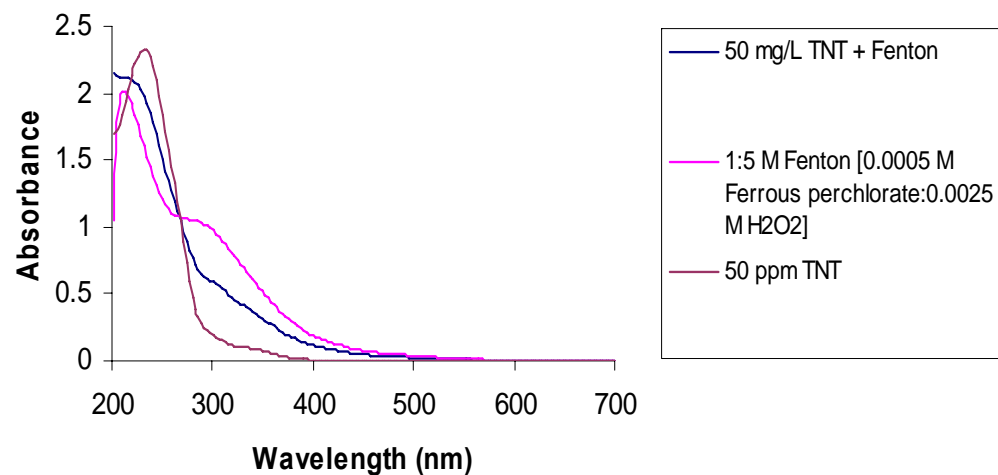


Free radical reactions cause no observable change in TNT

UV VIS Spectra of Irradiation of 50 mg/L TNT in water at 235 nm

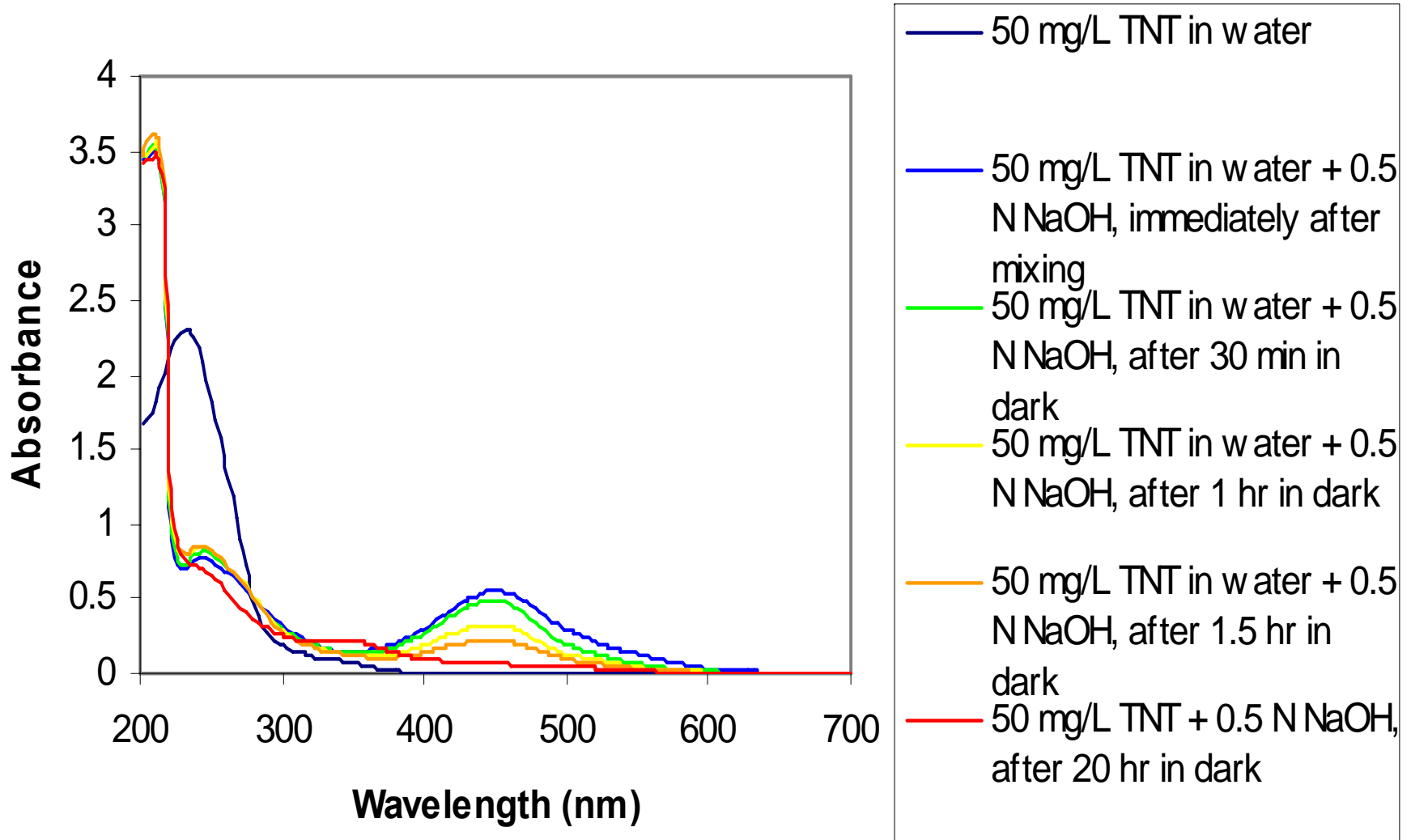


TNT + Fenton





UV VIS Spectra of 50 mg/L TNT + 0.5 N NaOH





Results – Nitramines/Cage Nitramines

US Army Engineer Research & Development Center

Irradiation of **CL-20** at λ_{\max} 233 nm resulted in a sharp, high-intensity peak characteristic of simple compounds and breaking of the rings

High concentration alkaline hydrolysis of **CL-20** results in a 3-member ring, recalcitrant pyrazine (shown in UV, SF spectra and DFT computational chemistry)

RDX and HMX transform easily upon irradiation at their respective λ_{\max}

RDX and HMX transform via alkaline hydrolysis only when high concentrations are used, similar to CL-20



One Corps, One Regiment, One Team . . . Serving Soldiers, the Army, the Nation



Results—Nitroaromatics (TNT)

US Army Engineer Research & Development Center

- Alkaline hydrolysis TNT results in generating a new absorption band at λ_{max} 450 nm. All absorption bands in the UV/Vis spectral region disappear, breaking the aromatic ring and suggesting transformation
- Free radical reactions via Fenton reagents and UV induced irradiation show no observable change in UV spectra



One Corps, One Regiment, One Team . . . Serving Soldiers, the Army, the Nation



Conclusions

US Army Engineer Research & Development Center

- Chemical transformation techniques must be selected according to molecular structure of the target compound
- Lower HOMO/LUMO values correlate with less polar, more symmetrical, higher number of C-C bonds
- Crowded compounds, resulting from increased number of nitro groups, are more susceptible to free radical reactions



One Corps, One Regiment, One Team . . . Serving Soldiers, the Army, the Nation



Acknowledgements

US Army Engineer Research & Development Center

- Semiempirical and spectroscopic experiments were conducted USACE ERDC, Environmental Lab, Vicksburg, MS
- DFT studies (tables not shown) were conducted at the Computational Center for Molecular Structure and Interactions, Jackson State University, MS
- We thank for their support:
 - Dr. John Cullinane, ERDC Technical Director
 - Dr. Richard E. Price, Environmental Division Branch Chief



One Corps, One Regiment, One Team . . . Serving Soldiers, the Army, the Nation



References

US Army Engineer Research & Development Center

- R. Bajpai, D. Parekh, S. Herrmann, M. Popović, J. Paca, M. Qasim; "A kinetic model of aqueous-phase alkali hydrolysis of 2,4,6-trinitrotoluene," *J. Haz. Materials* 106B (2004) 55-66.
- Y. Kholod, S. Okovytyy, G. Kuramshina, M. Qasim, P. Honea, J. Furey, H. Fredrickson, J. Leszczynski, "Are 1,5- and 1,7-dihydrodiimidazo[4,5-b:4',5'-e]pyrazine the main products of 2,4,6,8,10,12-hexanitro-2,4,6,8,10,12-hexaazaisowurtzitane (CL-20) alkali hydrolysis? A DFT Study of Vibrational Spectra,," *Journal of Molecular Structure* 794 (2006) 288-302.
- S. Okovytyy, Y. Kholod, M. Qasim, H. Frederickson, J. Leszczynski "The Mechanism of Unimolecular Decomposition of CL-20 (2,4,6,8,10,12 Hexanitro-2,4,6,8,10,12-Hexaazaisowurtzitane). A Computational DFT Study," *Journal of Physical Chemistry A* , 2005, 109, 2964-2970.
- M. Qasim, J. Furey, H. Fredrickson, J. Szecsody, C. McGrath, R. Bajpai, "Semi empirical Predictions of Chemical Degradation Reaction Mechanisms of CL-20 as Related to Molecular Structure," *Structuiral Chemistry*, Vol. 15, No. 5, 10/04.
- M. Qasim, H. Fredrickson, C. McGrath, J. Furey, R. Bajpai; "Theoretical Predictions of Chemical Degradation Reaction Mechanisms of RDX and Other Cyclic Nitramines Derived from Their Molecular Structures," *SAR/QSAR in Environmental Reearch*, Vol. 16, No. 3, 2005, 1-17.
- M. Qasim, H. Fredrickson, P. Honea, J. Furey, J. Leszczynski, S. Okovytyy, J. Szecsody, Y. Kholod; "Prediction of CL-20 Chemical Degradation Pathways, Theoretical and Experimental Evidence for Dependence on Competing Modes of Reaction," *SAR and QSAR in Environmental. Research*, Vol. 16, No. 5, 10/05, 493-515.



One Corps, One Regiment, One Team . . . Serving Soldiers, the Army, the Nation